Scientific Research Publishing

Advances in Materials Physics and Chemistry, 2024, 14, 55-65
https://www.scirp.org/journal/ampc
ISSN Online: 2162-5328
ISSN Print: 2162-531X

Study the Effect of Thickness on the Performance of PM6:Y6 Organic Solar Using SCAPS Simulation

Nagwa Ibrahim Mohammed Ibrahim[1], Amnah Mohammed Elharbi[2], Abdulrahman Albadri[3]

[1]Department of Physics, Science College, Qassim University, Buraydah, Saudi Arabia
[2]Department of Physics, Science College, Al Baha University, Baha, Saudi Arabia
[3]Microelectronics and Semiconductors Institute, King Abdulaziz City for Science and Technology, Riyadh, Saudi Arabia
Email: Arabia.nagwa.ib@qu.edu.sa, Amalharbi@bu.edu.sa, aalbadri@kacst.edu.sa

How to cite this paper: Ibrahim, N.I.M., Elharbi, A.M. and Albadri, A. (2024) Performance of PM6:Y6 Organic Solar Using SCAPS Simulation. *Advances in Materials Physics and Chemistry*, **14**, 55-65.
https://doi.org/10.4236/ampc.2024.144005

Received: March 28, 2024
Accepted: April 26, 2024
Published: April 29, 2024

Abstract

In this study, organic solar cells (OSCs) with an active layer, a blend of polymer of non-fullerene (NFA) Y6 as an acceptor, and donor PBDB-T-2F as donor were simulated through the one-dimensional solar capacitance simulator (SCAPS-1D) software to examine the performance of this type of organic polymer thin-film solar cell by varying the thickness of the active layer. PFN-Br interfacial layer entrenched in OPV devices gives overall enhanced open-circuit voltage, short-circuit current density and fill factor thus improving device performance. PEDOT: PSS is an electro-conductive polymer solution that has been extensively utilized in solar cell devices as a hole transport layer (HTL) due to its strong hole affinity, good thermal and mechanical stability, high work function, and high transparency in the visible range. The structure of the organic solar cell is ITO/PEDOT: PSS/BTP-4F: PBDB-T-2F/PFN-Br/Ag. Firstly, the active layer thickness was optimized to 100 nm; after that, the active-layer thickness was varied up to 900 nm. The results of these simulations demonstrated that the active layer thickness improves efficiency significantly up to 500 nm, then it decreased with increasing the thickness of the active layer from 600 nm, also notice that the short circuit current and the fill factor decrease with increasing the active layer from 600 nm, while the open voltage circuit increased with increasing the thickness of the active layer. The optimum thickness is 500 nm.

Keywords

Organic Solar Cells, PEDOT:PSS, BTP-4F (Y6), PBDB-T-2F (PM6), PFN-Br,

SCAPS 1D

1. Introduction

Organic solar cells (OSCs) are regarded as a promising technology for the commercialization of solar energy conversion due to their appealing features, such as their low weight, low cost, and the ability to produce large-area devices using solution casting techniques on mechanically flexible substrates [1] [2] [3]. The PEDOT: PSS and PFN-Br represent the electron and the hole transport layers (ETL and HTL). The PEDOT: PSS has high transparency in the visible region, good thermal stability, high mechanical stability, strong hole affinity and high work function [4], while the PFN-Br (PFN-Br) is used as anode and cathode interfacial materials, resulting in a promising PCE of 9.12% for a typical device with good stability [5]. The hole transport layers (HTL) make it easier for the positive charge carriers, or holes, which are produced when light is absorbed in the active layer to flow toward the anode. These layers typically comprise substances that are well suited to work with the layers next to them and that can move holes quickly. Conversely, the electron transport layer (ETL) facilitates the transfer of negative charge carriers, or electrons, produced in the active layer to the cathode [6] [7] [8].

Organic semiconductors have a relatively high exciton binding energy of several hundreds of mV, in contrast to traditional inorganic semiconductors [9] [10]. This is mostly due to the strong electron-hole interaction caused by a relatively low dielectric constant. Because of this, the production of free charges in ordered organic semiconductors is highly inefficient, and high temperatures and electric fields are needed to effectively separate excitons into charges [11]. Forming a so-called type II heterojunction—a combination of two materials with suitable energy level offsets—is one method to get past this issue [12]. The electron and hole frontier orbitals in this instance exhibit a parallel energy offset at the contact. Consequently, one of the components (the donor D) will donate a photoexcited electron to the second component (the acceptor A), or the other way around.

BTP-4F (Y6) is a non-fullerene acceptor or n-type organic semiconductor as shown in **Figure 1**. The absorption of BTP-4F is 600 nm - 1000 nm in the region corresponding to the near-infrared region, the absorption coefficient of BTP-4F is 821 nm [11], and its band gap is 1.4 eV [13]. PBDB-T-2F (PM6) is one member of the PBDB-T family and it is used as a donor polymer for the Polymer solar cells [14]. The HOMO/LUMO energy levels are pulled in PBDB-T by adding two fluorine atoms to each thiophene unit of the benzodithiophene (BDT) side chains as shown in **Figure 2**. Its absorption range is between 400 nm to 600 nm, and with an optical band gap of 1.80 eV [13]. One of the primary causes of the high JSC in OSC is that the two materials (BTP-4F, PBDB-T-2F) fully use the photons in the solar radiation spectrum [14].

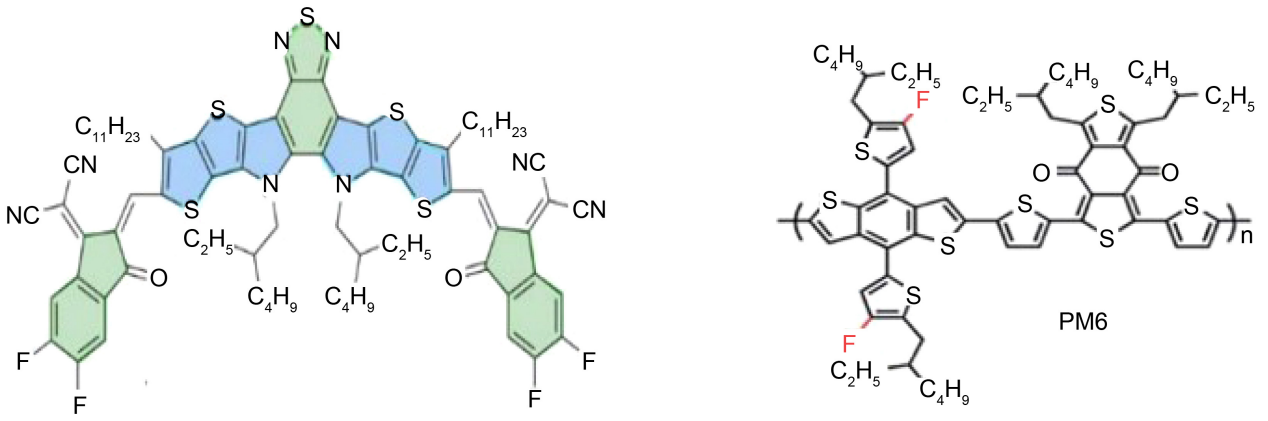

(a) (b)

Figure 1. The chemical structure of (a): BTPY-4F (Y6), (b): PBDB-T-2F (PM6).

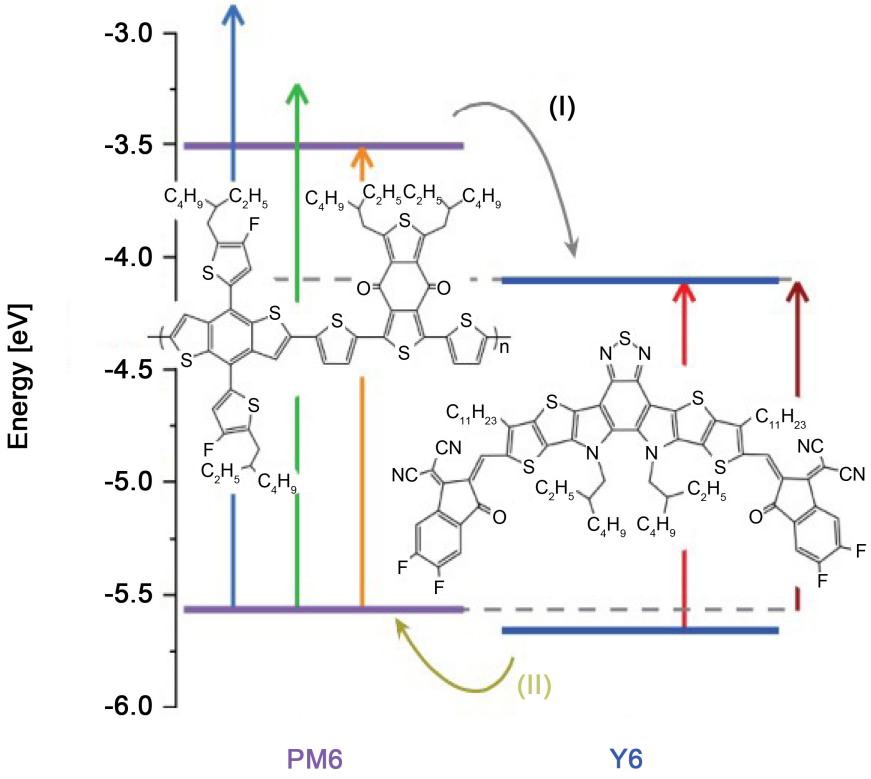

Figure 2. Chemical structure of PM6 and Y6 and energy levels.

2. Materials & Methods

2.1. Materials

ITO/PEDOT: PSS/PBDB-T-2F: BTP-4F/PFN-Br/Ag is the configuration of the simulated BHJ-OSC, PFN-Br is the electron transport layers ETL, PEDOT: PSS is the hole transport layers HTL, PBDB-T: BTP-4F is the active layer, ITO is the front contact, and Ag is the back contact. The fundamental structure of the simulated cell, as well as the other levels, are depicted in **Figure 3**.

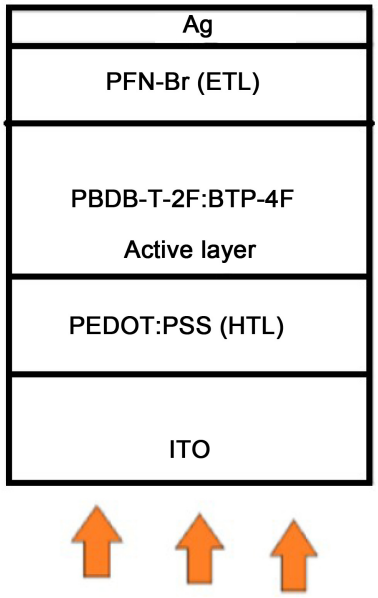

Figure 3. The fundamental structure of the simulated cell.

2.2. Methods

The SCAPS software (3.3.09) was used to carry out the simulation. This one-dimensional solar cell simulator was created by the University of Gent in Belgium. SCAPS 1D simultaneously solves many important semiconductor photovoltaic equations for the electron and hole separately, such as the continuity equation, Poisson equations, charge transport equations, diffusivity equations, and optical absorption equations. These formulas use geometrical and physical characteristics associated with each layer to calculate the total photovoltaic response of the designated solar cell [16].

Table 1 lists the numerical parameters that were used to execute the SCAPS simulation. Consequently, measurements of photovoltaic characteristics were made, including power conversion efficiency (PCE), fill factor (FF), open-circuit voltage (Voc), and short circuit current density (Jsc). Figure 4 shows a J-V curve that is lit.

3. Results and Discussions

3.1. Results

Table 1 displays the important physical characteristics of the solar cell layers as defined by the simulation. Energy band gap is represented by E_g, relative permittivity by ε_r, electron affinity by χ, electron and hole mobility by μ_n and μ_p. The effective DOS of the valence and conduction bands are N_c and N_v, respectively, while the densities of the donor and acceptor materials are N_D and N_A [17]. The work function for Ag is 4.1 eV, Ag used as a back contact [16], ITO with work function of 4.2−5eV, used as a front contact [18].

$J-V$ characteristic of the simulated device. $J-V$ curves are the parameters

Table 1. Parameters used in the SCAPS-1D software [2] [15] [16] [17] [24] [25] [26].

Parameters	PEDO: PSS	PBDB-T-2F: BTP-4F (Active layer)	PFN-Br (ETL)
Thickness (nm)	40	50 - 1450	10
χ (eV)	3.4	4.03	4
E_g (eV)	1.6	1.27	2.98
ε_r (primitivity)	3	6.1	5
N_c (cm^3)	1×10^{22}	1×10^{19}	1×10^{19}
N_v (cm^3)	1×10^{22}	1×10^{19}	1×10^{19}
μ_p	9.9×10^{-5}	2.96×10^{-4}	1×10^{-4}
μ_n	4.5×10^{-4}	1.7×10^{-3}	2×10^{-6}
N_A (cm^{-3})	0	0	0
N_D (cm^{-3})	2×10^{18}	7.5×10^{16}	9×10^{18}

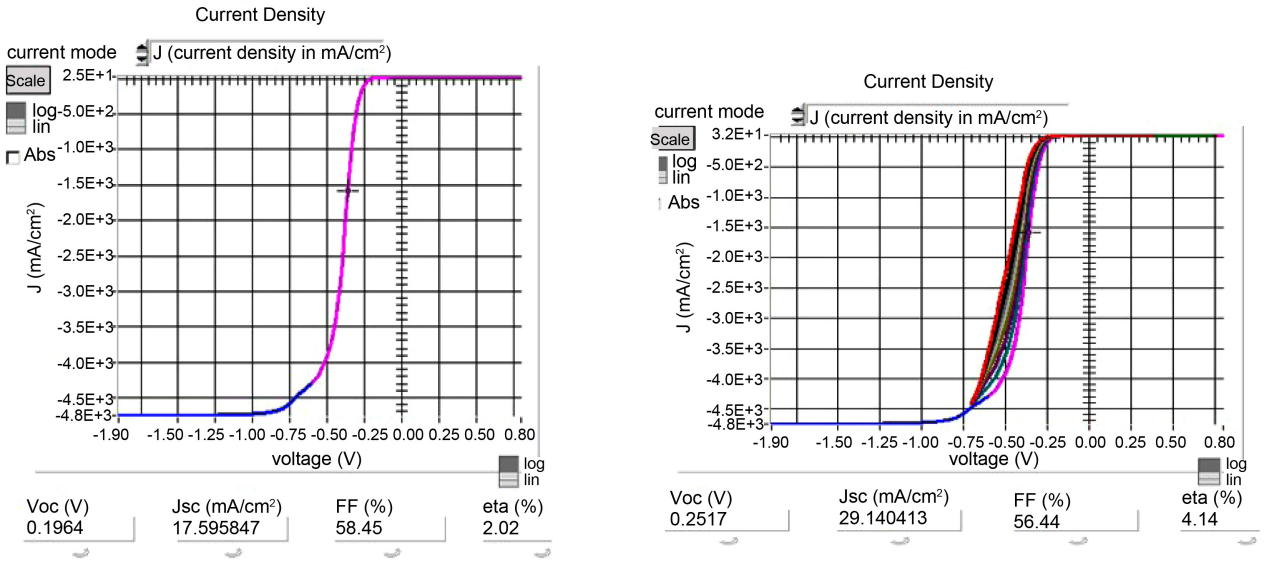

(a) (b)

Figure 4. (a): $J-V$ characteristic of the simulated device for the thickness of 100 nm. (b): $J-V$ characteristic of the simulated device for the thickness of 500 nm.

used to calculate the electrical output power of solar cells. Figure 4 shows the $J-V$ curve of the hybrid simulated device for 100 nm layer thickness. The thickness changes from 100 nm to 900 nm. The solar cells are output parameters under the standard simulated sunlight of AM1.5G. The working condition is at ambient temperature and frequency of 106 Hz. In Figures 5-8, the effect of the thickness variation on the efficiency, fill factor, short-circuit current, and open circuit voltage is illustrated using SCAPS Simulation, that govern the device's $J-V$ properties, taking into account the layer thicknesses explicitly. This comprehensive technique enables us to calculate how much material mobility should be improved and/or the recombination coefficient reduced in PM6:Y6 thick-junction

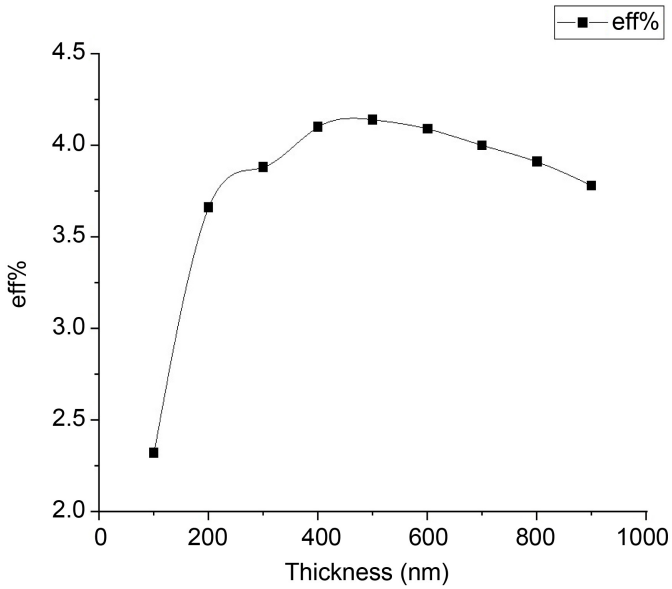

Figure 5. The effect of the thickness of active layer on the efficiency of solar cell.

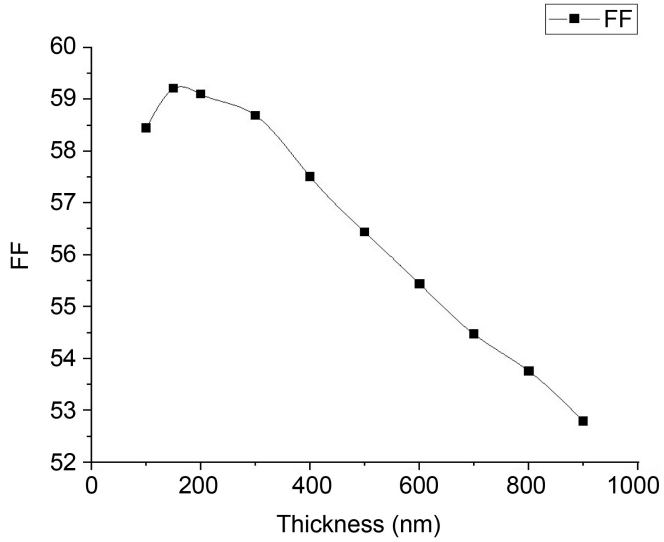

Figure 6. The effect of the thickness of active layer on the fill factor.

devices in order to achieve the parameters that affect the performance of the solar cells. The device with the optimal thickness is found to be 500 nm. The device VOC and JSC (0.251 V and 29.14, respectively) have little thickness dependence. We just determined that the invariant JSC is due to Y6's extremely long diffusion length [19]. On the other hand, the VOC trend is fairly typical [20] and hence will not be examined further. As an example, introducing fullerene PCBM to a PM6/Y6 blend resulted in a significant improvement in both hole and electron mobilities [21]. This is consistent with past cases of adding PCBM to NFA-based solar cells, which resulted in better mobilities and device performance [22]. However, little is known about how such changes in morphological features

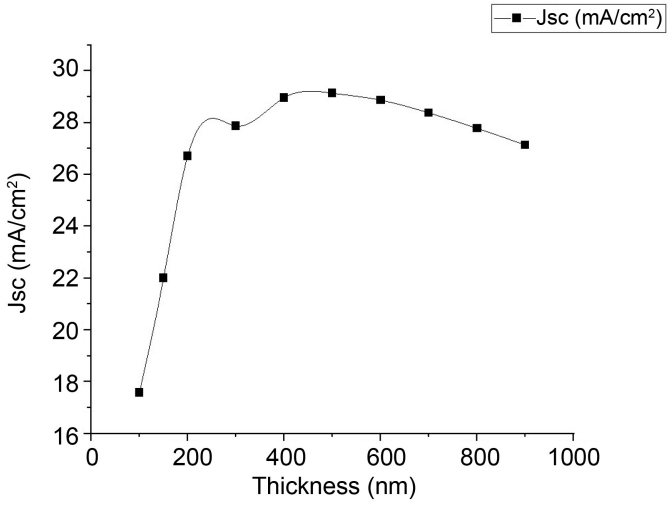

Figure 7. The effect of the thickness of active layer on the short density current.

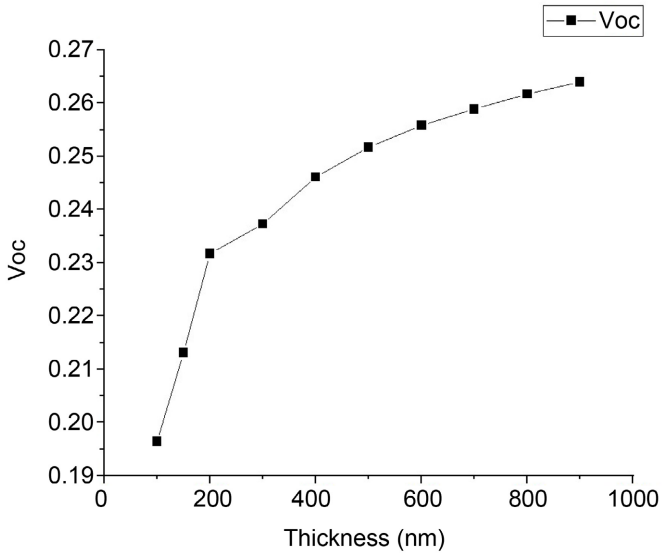

Figure 8. The effect of the thickness of active layer on the open circuit voltage.

affect the energy landscape of the mix and the competition between charge extraction and recombination. Furthermore, the optical and electrical contribution of the third component to the binary BHJ makes comprehension challenging. Thus, motivated by these findings and our understanding of the significance of molecular additives, which can increase polymer crystallization and packing [23], we modified the percentage of the integrated molecular component in the mix for various junction thicknesses.

3.2. Discussions

The inverted devices were approximated with the glass/indium tin oxide (ITO), PEDOT: PSS/active layer/PFN-Br/Ag structure. The peak light absorption range

is the primary consideration when selecting new materials. Specifically, in PEDOT: PSS electrodes, the highest occupied molecular orbital HOMO energy level is around 5.0 to 5.3 eV and the lowest unoccupied molecular orbital LUMO energy level is around 2.2 eV, which increased the performance of the solar cells by facilitating hole injection, PM6 between 550 nm and 650 nm, and Y6 between 750 nm and 850 nm. The active layer in the blue visible range increases the device's overall absorption spectrum coverage. The lowest unoccupied molecular orbital LUMO energy levels of PEDOT: PSS, PM6, and Y6 are −2.2 eV, −3.75 eV, and −4.09 eV, respectively. The equivalent the highest occupied molecular orbital HOMO energy levels are −5.3 eV, −5.50 eV, and −5.61 eV. This configuration creates a trapezoidal structure, which improves the transit efficiency of free electrons and holes after exciton dissociation. Notably, Y6 has a higher lowest unoccupied molecular orbital (LUMO) energy level than PM6, resulting in a stronger built-in electric field at the device heterojunction and so reducing electron-hole recombination [24] [27] [28] [29].

Under simulated AM 1.5G light, the results show that **Figure 4(a)** and **Figure 4(b)** display the current density–voltage ($J-V$) curves for the 100 and 500 nm thick PM6:Y6. At the thickness of 500 nm, the device displays 4.1% PCE, a VOC of 0.25 V, a JSC of 29.14 mA/cm^2, and an FF of 56.44.4%. **Figure 5** clear increase in efficiency response between 100 nm to 500 nm was observed when the active layer increases (**Figure 5**) by increasing the thickness of the active layer of our solar cells, the short circuit current and the efficiency increase up to 500 nm, then they began to decreases slightly. To be more precise, the short-circuit current density rises to 29.14 mA/cm^2 from 17.39 mA/cm^2 and then marginally falls to 27.4 mA/cm^2 **Figure 7**. The main reason for this is a thickness increase, which raises the mobility of free electrons and holes and increases the efficiency of exciton dissociation. nevertheless, also raising, raising the exciton recompilations [30]. The open circuit voltage increases by increasing the active layer of the solar cells. As the thickness of the active layer increases, the decrease in FF is mainly caused by an increase in series resistance. The decrease in the FF can be explained, as has been previously mentioned in the literature, by higher bimolecular recombination losses [31] [32] during charge transport or space charge effects, which can be brought on by imbalanced carrier mobilities or increasing the thickness of the active layer [15] [33] [34]. Charge carrier entrapment, the longer distance charge carriers must travel, and an increase in resistance losses within the device are all responsible for this rise in resistance losses.

4. Conclusion

ITO/PEDOT: PSS/BTP-4F: PBDB-T-2F/PFN-Br/Ag bulk heterojunction solar cell is simulated for various active layer thicknesses (100 nm - 900 nm with a difference of 100 nm). The effect of the thickness of the active layer (BTP-4F: PBDB-T-2F) of the solar cell on the power conversion efficiency and the other electrical parameters such as open circuit voltage, short circuit current density

(Jsc, fill factor, and the open circuit voltage (Voc), is studied. It was observed that short circuit current density and power conversion efficiency increase with thickness up to 500 nm of the active layer thickness in simulated bulk heterojunction (BHJ) solar cells and thereafter decrease. The strong dependence of short circuit current density (Jsc) on power conversion efficiency is observed. The fill factor declines with increasing as thickness grows. This is due to charge recombination appears to decrease with thickness. Optimizing the thickness is necessary to get optimal efficiency.

Acknowledgements

I would like to express my special thanks of gratitude the Dean ship of Scientific Research Qassim University and King Abdulaziz City for Science and Technology National Semiconductor Center and Electronic for help us to finish this work.

Conflicts of Interest

The authors declare no conflicts of interest regarding the publication of this paper.

References

[1] Khan, M.R. and Jarzombek, B. (2023) Optimization and Efficiency Enhancement of Modified Polymer Solar Cells. *Polymers*, **15**, Article 3674. https://doi.org/10.3390/polym15183674

[2] Al-Muhimeed, T.I., Alahmari, S., Ahsan, M. and Salah, M.M. (2023) An Investigation of the Inverted Structure of a PBDB:T/PZT:C1-Based Polymer Solar Cell. *Polymers*, **15**, Article 4623. https://doi.org/10.3390/polym15244623

[3] Yung, F., Huang, Y., Li, Y. and Li, Y. (2021) Large-Area Flexible Organic Solar Cells. *npj Flexible Electronics*, **5**, Article No. 30. https://doi.org/10.1038/s41528-021-00128-6

[4] Wang, M., Zhou, M., Zhu, L., Li, Q. and Jiang, C. (2016) Enhanced Polymer Solar Cells Efficiency by Surface Coating of the PEDOT:PSS with Polar Solvent. *Solar Energy*, **129**, 175-183. https://doi.org/10.1016/j.solener.2016.02.003

[5] Wang, Y., Shi, Z., Liu, H., Wang, F., *et al.* (2017) The Effect of Donor and Norfullerene Acceptor Inhomogeneous Distribution within the Photoactive Layer on the Performance of Polymer Solar Cells with Different Device Structures. *Polymers*, **9**, Article 571. https://doi.org/10.3390/polym9110571

[6] Sharma, N., Gupta, S.K. and Singh Negi, C.M. (2019) Influence of Active Layer Thickness on Photovoltaic Performance of PTB7:PC70BM Bulk Heterojunction Solar Cell. *Superlattices and Microstructures*, **135**, Article 106278. https://doi.org/10.1016/j.spmi.2019.106278

[7] Ramírez-Como, M., Balderrama, V.S., Sacramento, A., Marsal, L.F., Lastra, G. and Estrada, M. (2019) Fabrication and Characterization of Inverted Organic PTB7:PC70BM Solar Cells Using Hf-in-ZnO as Electron Transport Layer. *Solar Energy*, **181**, 386-395. https://doi.org/10.1016/j.solener.2019.02.015

[8] Dridi, C., Touafek, N. and Mohamedi, R. (2022) Inverted PTB7:PC70BM Bulk Heterojunction Solar Cell Device Simulations for Various Inorganic Hole Transport

Materials. *Optik*, **252**, Article 168447. https://doi.org/10.1016/j.ijleo.2021.168447

[9] Bag, M., Kumar, J. and Kumar, R. (2023) Chapter 6—Polymer Semiconducting Materials for Organic Solar Cells. In: Khan, A., Nazim, M. and Asiri, A., Eds., *Advances in Electronic Materials for Clean Energy Conversion and Storage Applications*, Woodhead Publishing, Cambridge, United Kingdom, 123-148. https://doi.org/10.1016/B978-0-323-91206-8.00022-4

[10] Shehzad, R.A., Zahid, S., Rasool, A. and Iqbal, J. (2022) Organic Semiconductors for Photovoltaics. In: Gupta, R., Ed., *Handbook of Energy Materials*, Springer, Singapore, 1-33. https://doi.org/10.1007/978-981-16-4480-1_66-1

[11] Bratina, G. and Pavlica, E. (2019) Characterization of Charge Carrier Transport in Thin Organic Semiconductor Layers by Time-of-Flight Photocurrent Measurements. *Organic Electronics*, **64**, 117-130. https://doi.org/10.1016/j.orgel.2018.09.049

[12] Skromme, B.J. (2006) Semiconductor Heterojunctions. In: Jürgen Buschow, K.H., Cahn, R.W., Flemings, M.C., *et al*, Eds., *Encyclopedia of Materials*: *Science and Technology* (*Second Edition*), Pergamon Press, Oxford, 1-11. https://doi.org/10.1016/B0-08-043152-6/02083-0

[13] Zhong, S., Yap, B.K., Zhong, Z. and Ying, L. (2022) Review on Y6-Based Semiconductor Materials and Their Future Development via Machine Learning. *Crystals*, **12**, Article 168. https://doi.org/10.3390/cryst12020168

[14] Wang, Y., *et al*. (2017) High-Performance Nonfullerene Polymer Solar Cells Based on Fluorinated Wide Bandgap Copolymer with a High Open-Circuit Voltage of 1.04 V. *Journal of Materials Chemistry A*, **5**, 22180-22185. https://doi.org/10.1039/C7TA07785H

[15] Prajapati, U.K., Soni, E., Solanki, M. and Rani, J. (2023) Enhancing the Efficiency of PM6:Y6 Bulk-Heterojunction Organic Solar Cells through SCAPS Simulation Optimization. *Chinese Journal of Physics*. https://doi.org/10.1016/j.cjph.2023.12.028

[16] Mathur, A.S., Dubey, S., Nidhi, and Singh, B.P. (2020) Study of Role of Different Defects on the Performance of CZTSe Solar Cells Using SCAPS. *Optik*, **206**, Article 163245. https://doi.org/10.1016/j.ijleo.2019.163245

[17] Abdelaziz, W., Shaker, A., Abouelatta, M. and Zekry, A. (2019) Possible Efficiency Boosting of Non-Fullerene Acceptor Solar Cell Using Device Simulation. *Optical Materials*, **91**, 239-245. https://doi.org/10.1016/j.optmat.2019.03.023

[18] Schnippering, M., *et al*. (2007) Electronic Properties of Ag Nanoparticle Arrays. A Kelvin Probe and High Resolution XPS Study. *Physical Chemistry Chemical Physics*, **9**, 725-730. https://doi.org/10.1039/B611496B

[19] Philippa, B., Stolterfoht, M., Burn, P.L., Juška, G., Meredith, P., White, R.D. and Pivrikas, A. (2014) The Impact of Hot Charge Carrier Mobility on Photocurrent Losses in Polymer-Based Solar Cells. *Scientific Reports*, **4**, Article No. 5695. https://doi.org/10.1038/srep05695

[20] Shewchun, J., Dubow, J., Wilmsen, C.W., Singh, R., Burk, D. and Wager, J. (1979) The Operation of the Semiconductor-Insulator-Semiconductor Solar Cell: Experiment. *Journal of Applied Physics*, **50**, 2832-2839. https://doi.org/10.1063/1.326196

[21] Zhu, Y., Gadisa, A., Peng, Z., Ghasemi, M., Ye, L., Xu, Z., Zhao, S. and Ade, H. (2019) Rational Strategy to Stabilize an Unstable High-Efficiency Binary Nonfullerene Organic Solar Cells with a Third Component. *Advanced Energy Materials*, **9**, Article 1900376. https://doi.org/10.1002/aenm.201900376

[22] Singh, R., Lee, J., Kim, M., Keivanidis, P.E. and Cho, K. (2017) Control of the Molecular Geometry and Nanoscale Morphology in Perylene Diimide Based Bulk Heterojunctions Enables an Efficient Non-Fullerene Organic Solar Cell. *Journal of*

Materials Chemistry A, **5**, 210-220. https://doi.org/10.1039/C6TA08870H

[23] Amin, P.O., Muhammadsharif, F.F., Saeed, S.R. and Ketuly, K.A. (2023) A Review of the Improvements in the Performance and Stability of Ternary Semi-Transparent Organic Solar Cells: Material and Architectural Approaches. *Sustainability*, **15**, Article 12442. https://doi.org/10.3390/su151612442

[24] Bhujel, R., Rai, S., Deka, U., Sarkar, G., Biswas, J. and Swain, B.P. (2021) Bandgap Engineering of PEDOT:PSS/rGO a Hole Transport Layer for SiNWs Hybrid Solar Cells. *Bulletin of Materials Science*, **44**, Article No. 72. https://doi.org/10.1007/s12034-021-02376-8

[25] Zhang, S., Ye, L., Zhao, W., Yang, B., Wang, Q. and Hou, J. (2015) Realizing over 10% Efficiency in Polymer Solar Cell by Device Optimization. *Science China Chemistry*, **58**, 248-256. https://doi.org/10.1007/s11426-014-5273-x

[26] Tomblaine, N., *et al*. (2020) Extraordinarily Long Diffusion Length in PM6:Y6 Organic Solar Cells. *Journal of Materials Chemistry A*, **8**, 7854-7860. https://doi.org/10.1039/D0TA03016C

[27] Yang, J., *et al*. (2023) Improved Short-Circuit Current and Fill Factor in PM6:Y6 Organic Solar Cells through D18-Cl Doping. *Nanomaterials*, **13**, Article 2899. https://doi.org/10.3390/nano13212899

[28] Ma, J.H., *et al*. (2023) Highly Efficient ITO-Free Quantum-Dot Light Emitting Diodes via Solution-Processed PEDOT:PSS Semitransparent Electrode. *Materials*, **16**, Article 4053. https://doi.org/10.3390/ma16114053

[29] Jäckle, S., Liebhaber, M., Gersmann, C., Mews, M., Jäger, K., Hristiansen, S. and Lips, K. (2017) Potential of PEDOT:PSS as a Hole Front Contact for Silicon Heterojunction Solar Cells. *Scientific Reports*, **7**, Article No. 2170. https://doi.org/10.1038/s41598-017-01946-3

[30] Yu, K., *et al*. (2022) 18.01% Efficiency Organic Solar Cell and 2.53% Light Utilization Efficiency Semitransparent Organic Solar Cell Enabled by Optimizing PM6:Y6 Active Layer Morphology. *Science China Chemistry*, **65**, 1615-1622. https://doi.org/10.1007/s11426-022-1270-5

[31] Nomin, M., *et al*. (2021) Requirements for Making Thick Junctions of Organic Solar Cells Based on Norfullerene Acceptors. *Solar RRL*, **5**, Article 2100018. https://doi.org/10.1002/solr.202100018

[32] Wang, K., *et al*. (2021) Enhanced Short Circuit Current Density and Efficiency of Ternary Organic Solar Cells by Addition of a Simple Copolymer Third Component. *Chemical Engineering Journal*, **425**, Article 130575. https://doi.org/10.1016/j.cej.2021.130575

[33] Jia, Z., Qin, S., Meng, L., Ma, Q., Angunawela, I., Zhang, J., Li, X., He, Y., Lai, W., Li, N., *et al*. (2021) High Performance Tandem Organic Solar Cells via a Strongly Infrared-Absorbing Narrow Bandgap Acceptor. *Nature Communications*, **12**, Article No. 178. https://doi.org/10.1038/s41467-020-20431-6

[34] Chen, W.Q. and Zhang, Q.C. (2017) Recent Progress in Non-Fullerene Small Molecule Acceptors in Organic Solar Cells (OSCs). *Journal of Materials Chemistry C*, **5**, 1275-1302. https://doi.org/10.1039/C6TC05066B